Available online at www.sciencedirect.com
SCIENCE DIRECT®
Journal of Nuclear Materials 343 (2005) 267–274
journal of nuclear materials
www.elsevier.com/locate/jnucmat

LiSoR irradiation experiments and preliminary post-irradiation examinations

H. Glasbrenner *, Y. Dai, F. Gröschel

Paul Scherrer Institut (PSI), Spallation Neutron Source Division, CH-5232 Villigen, PSI, Switzerland

Abstract

The LiSoR (Liquid metal–Solid metal Reaction) facility was developed and installed to investigate especially the effects of liquid metal corrosion and embrittlement under irradiation. LiSoR setup is basically a LBE loop with a test section irradiated with 72 MeV protons whereby so far four test sections including T91 specimens have been irradiated in the presence of flowing LBE.

Post-irradiation examinations (PIE) have been started up to now only on the test section irradiated for 34 h. Optical microscopy, scanning electron microscopy and micro-hardness tests have been completed on both the tube and tensile specimen in the test section. On the surfaces of the tensile specimen, LBE wetting was observed in the irradiated area and the area immediate above the irradiated zone. Below the irradiated area some depositions are observed on the surfaces. A thin oxide layer of about 3 μm was formed in the irradiated area only and no oxide layer is revealed above or below that region. Additionally, in the area above the irradiated area, slight dissolution is observed on the surface due to the absence of a protecting oxide layer.

In this paper a summary of the LiSoR irradiation experiments carried out up to now are presented and as well the first results on PIE revealed on the test section irradiated for 34 h.

1. Introduction

Lead-bismuth eutectic (LBE) alloy is beside lead one of the prime candidates to be applied as target material for a future accelerator driven system (ADS) reactor. Beside many attractive features of LBE concerning physical properties like low vapour pressure, extremely small neutron absorption cross-section and a high yield of about 28 n per 1 GeV proton, little moderation of neutrons and very low melting point (T_m = 123.5 °C) one has to keep in mind that the interaction of structural materials with LBE has to be investigated under very specific conditions. It is well-known that liquid metal corrosion and/or liquid metal embrittlement (LME) may occur dependent on different parameters: type of steel plays a role and as well the thermal conditioning, surface treatment of the steel, temperature and velocity of LBE and oxygen content in LBE.

Meanwhile the mechanism responsible for liquid metal corrosion is relatively well understood in lead and lead-bismuth and thus special features exist helping to suppress it [1–4]. On the other hand it is not so easy to predict if liquid metal embrittlement might happen. LME can lead to a severe and very fast usually brittle inter-granular failure of the ductile structural material [5,6]. Although the phenomenon of LME has been

* Corresponding author. Tel.: + 41 56 310 4712; fax: + 41 56 310 2199.
E-mail address: heike.glasbrenner@psi.ch (H. Glasbrenner).

0022-3115/$ - see front matter © 2005 Elsevier B.V. All rights reserved.
doi:10.1016/j.jnucmat.2004.08.031

recognized for many years, its explanation has not yet emerged and is prediction is lacking. There is some work ongoing in Europe trying to understand LME and a lot of effort is still given to liquid metal corrosion without irradiation.

Due to the good mechanical properties of ferritic martensitic steels under irradiation they are under consideration as tentative materials for the liquid metal containers of high power spallation targets [7,8]. Latest investigations performed on ferritic-martensitic steel (mainly T91) and LBE revealed that this kind of steels can show LME [9–12]. If one is not willing to disclaim on ferritic-martensitic steels due to the good behaviour under irradiation the best way would be to protect the surface of the steel to prevent LME.

The influence of irradiation, the spallation products generated during irradiation and the change in the micro structure as consequence of irradiation could affect the interaction of steel with LBE concerning liquid metal corrosion and LME. Therefore it is urgently required to perform irradiation experiments with steel in the presence of LBE to proof whether Liquid metal–Solid metal Reactions (LiSoR) are enhanced under irradiation in the presence of mechanical stress. Since this is a question that must be answered before a liquid metal target can be used in a spallation neutron source, the LiSoR experiment has been initiated to use 72 MeV protons generated by the Philips cyclotron at PSI to irradiate stressed steel specimens in contact with flowing liquid metal.

Up to now four irradiation experiments were performed in the LiSoR installation and first post-irradiation examinations (PIE) have been started.

2. Experimental

2.1. LiSoR loop

The loop is fabricated of the austenitic steel 316L. About 18 l of LBE were filled into the loop and approximately 15 l are pumped around during operation. The loop is equipped with an electromagnetic induction pump and a flow meter (both constructed at IPUL, Riga). Heat exchanger system LBE – oil/oil – water/water – water was installed to the loop. The operation of the loop is completely automatically. In total 4 test sections were irradiated up to now. Further details concerning the loop, components and the test sections are described elsewhere [13,14].

2.2. Materials

Test section no. 1 made of martensitic MANET II steel was fabricated by ATEA, France. The MANET II steel was supplied as rod material with 95 mm in diameter in standard heat treated conditions (1075 °C 30 min/750 °C 2 h) by company Saarstahl-Völklingen, Germany (charge no. 50757). The chemical composition of MANET II in wt% is 10.3 Cr, 0.65 Ni, 0.57 Mo, 0.28 Si, 0.96 Mn, 0.11 C, 0.21 V, 0.007 P, 0.15 Nb and with Fe in balance. Test sections nos. 2, 3 and 4 made of the ferritic steel T91 were manufactured in total by company SOTEREM, France. All specimens to be irradiated are as well made of ferritic steel T91. The T91 steel used for the tubes was purchased from Creusot Loire Industrie (France) and has a composition in wt% of 8.26 Cr, 0.13 Ni, 0.95 Mo, 0.43 Si, 0.38 Mn, 0.1 C, 0.2 V, 0.017 P, 0.065 Nb and with Fe in balance. While the T91 steel used for the tensile specimens was obtained from SPIRE program produced by Ugine (France) and has a composition in wt% of 8.63 Cr, 0.23 Ni, 0.95 Mo, 0.31 Si, 0.43 Mn, 0.1 C, 0.21 V, 0.02 P, 0.09 Nb and with the balance Fe. Both materials have the standard heat treatment, namely normalized at 1040 °C for 1 h followed by air cooling, and then tempered at 760 °C for 1 h followed by air cooling. The outer surfaces of the tube were milled and the inner surfaces were cut with an electron discharging machine. Test section nos. 1 and 2 were irradiated without any further polishing of the inner and outer surfaces. The inner surfaces of the tubes of test section nos. 3 and 4 were mechanically polished by hand in order to produce a smooth and uniform surface without any cracks. The tensile specimens were cut by an electron discharging machine. Its surfaces were polished mechanically with SiC grinding papers.

Company Impag AG (Switzerland) supplied the eutectic Pb-55.5Bi (44.8 Pb and 55.2 Bi wt%) alloy which contained as less as only a few ppm of impurities: Ag 11.4, Fe 0.78, Ni 0.42, Sn 13.3, Cd 2.89, Al 0.3, Cu 9.8, Zn 0.2, wt%.

2.3. Dimensions of the specimens

The dimensions of the flat bar tensile specimen tested in test section no. 1 under irradiation are the following: 5 mm in diameter, 20 mm of gauge length, 1 mm thickness of the plate and 35 mm distance between the shoulders. Photograph of the specimen is given in Fig. 1.

The specimens irradiated in test section nos. 2, 3, 4 were prepared in the dimensions shown in Fig. 2. The orientation of the specimens in the plate is parallel to the rolling direction. In order to investigate the influence of irradiation on a weld near the beam zone, an electron-beam weld was introduced in the specimen. After welding the gauge area of the specimen was re-heat-treated to 740 °C for 120 min in order to relieve the welding stresses. The gauge area was mechanically polished and finished with polishing papers of no. 2000 to get a smooth surface. The specimens were degreased with ethanol and acetone before installation into the according LiSoR test section.

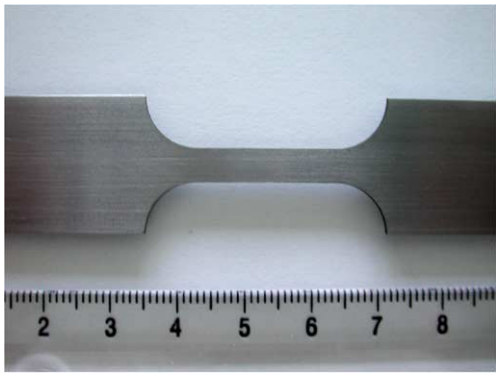

Fig. 1. Photograph of the tensile specimen ruptured during the first irradiation experiment.

2.4. Irradiation experiments

Up to now four irradiation tests have been performed. The parameters chosen for these experiments are summarised in Table 1. Mechanical testing was performed on T91 specimen during the first irradiation performed in test section no. 1, having a tube made of MANET II steel instead of T91. The specimen was exposed to flowing LBE at 300 °C for 24 h, in addition the specimen was irradiated for 1 h (i.e. after 23 h of exposure) before the tensile test was performed under irradiation. For comparison another tensile test was carried out under the same conditions but without irradiation.

Before irradiation of test section nos. 2, 3 and 4 was started T91 specimens were stressed in tension to 200 MPa (which corresponds to a load of 4000 N). Irradiation experiments nos. 2, 3 and 4 have to be stopped ahead of schedule. The reasons stopping irradiation of test section no. 2 was a crack in the beam window hence LBE dropped out [15]. Irradiation experiments of test sections nos. 3 and 4 have to be interrupted ahead of schedule because the leak sensor in the beam line has indicated wrongly a leakage. Optical inspection of the beam windows after dismantling showed no leakage or crack [16]. Due to the false signal of the leak sensor of test section no. 3 a modified version was constructed and used in test section no. 4. Detailed PIE of test sections and specimens of irradiation nos. 3 and 4 will soon be started.

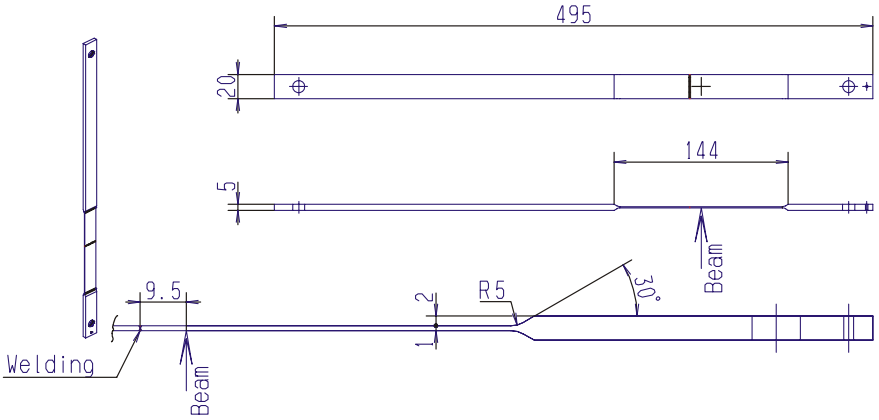

Fig. 2. Nominal dimensions of the welded specimen irradiated in test section nos. 2, 3 and 4.

Table 1
The various parameters used for the four different irradiation experiments are summarised

Test section	No. 1	No. 2	No. 3	No. 4
Beam energy on target	72 MeV	72 MeV	72 MeV	72 MeV
Beam current	50 μA	50 μA	15 μA	30 μA
Beam profile on target (gaussian)	$\sigma_x = \sigma_y = 0.8$ mm	$\sigma_x = \sigma_y = 0.8$ mm	$\sigma_x = \sigma_y = 1.6$ mm	$\sigma_x = \sigma_y = 1.2$ mm
Beam wobbling max frequency	14.3 Hz in X, 1.19 Hz in Y (12:1)	14.3 Hz in X, 1.19 Hz in Y (12:1)	14.3 Hz in X, 2.38 Hz in Y (6:1)	14.3 Hz in X, 2.38 Hz in Y (6:1)
Time of irradiation	1 h	34 h	264 h	144 h
Irradiation dose	~0 dpa	0.1 dpa	0.2 dpa	0.2 dpa

2.5. Examination of tensile specimens exposed to LBE in test section no. 1

Visual examination, optical microscopy, scanning electron microscopy (SEM) and EDX was performed on the fracture faces of the T91 specimens ruptured with and without irradiation. The MANET II tube of the test section was inspected as well in the irradiated zone and next to it by the methods mentioned above and in addition Vickers micro hardness measurements were performed.

2.6. Examination of LBE, test section tube and specimen after irradiation no. 2

Visual examination, optical microscopy, scanning electron microscopy (SEM) and micro-hardness tests have been performed on both the tube and tensile specimen in the test section.

Analysis on irradiated LBE sipped out of the crack in the tube was done in order to reveal the Po isotopes generated during irradiation. To distinguish between different Po-isotopes (e.g. ^{206}Po, ^{208}Po, ^{210}Po) by high-resolution α-spectroscopy, quantitative radiochemical separation methods had to be applied and are described elsewhere [17]. The FLUKA Monte Carlo code [18] was used to simulate the experiment. Production rates of the residual nuclei produced during irradiation were generated and written to a file. These production rates were then read and processed using the ORIHET3 code [19] which performs the build up of the radionuclide inventory during the irradiation time.

3. Results obtained for test section no. 1 and discussion

3.1. MANET II tube after irradiation

There is no difference visible between the irradiated and the non-irradiated zone on the MANET II tube. Hence in the following there will be made no differentiation and the results revealed apply for both areas. The inner surface is not uniform and many micro cracks parallel and perpendicular to the surface are visible as can be seen in Fig. 3. The roughness of the surface and the cracks were produced during fabrication by EDM wire cutting. It was neglected to rework the inner surface of the tube to get a smooth crack free surface. The Vicker micro hardness measured in the MANET II specimens were between 275 and 288 HV0.05 independent on the position (irradiated or unirradiated area). There was no hardening of the steel measurable due to the short irradiation period of only 1 h. The optical microscopy on the polished cut of the inner surface of the MANET II tube revealed an oxide layer which varies in thickness between approximately 3 and 7 μm and having a two-layered structure: the outer layer mainly consists of the compound Fe_3O_4, the oxide layer staying in contact with the basic material is formed by the spinel type $Fe(Fe_{1-x}Cr)_2O_4$. EDX analysis could not be performed on the irradiated area due to the quite high activity (4 mSv/h in contact) which makes this kind of analysis impossible. The EDX point analysis of the unirradiated area showed that the content of Pb is relatively high in the oxide layer. The element Bi is as well present in this layer but compared to the ratio in LBE it is downgraded (ratio in LBE: Pb/Bi = 0.8, in the oxide layer: Pb/Bi = 4.4). Probably Pb diffuses preferred into the oxide layer in opposition to Bi. One reason for the contrary diffusion behaviour of Pb and Bi could be their crystal structures. Bi crystallises rhombic face centred and Pb face centred cubic (fcc). The O^{2-} ions in the compounds Fe_3O_4 and $Fe(Fe_{1-x}Cr)_2O_4$ crystallise as well in fcc structure.

3.2. T91 tensile specimens

There was no difference of the rupture behaviour observable between the irradiated and the unirradiated tensile specimens. The fracture mode on both specimens

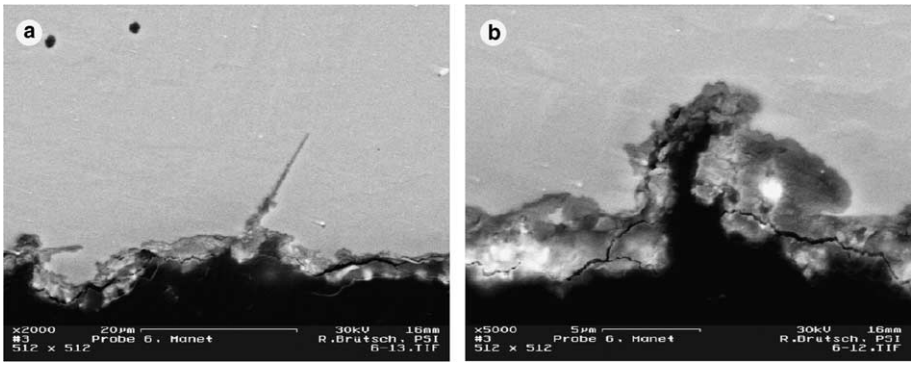

Fig. 3. SEM images of the unirradiated zone showing the oxide layer on the rough inner surface with some cracks of the MANET II tube.

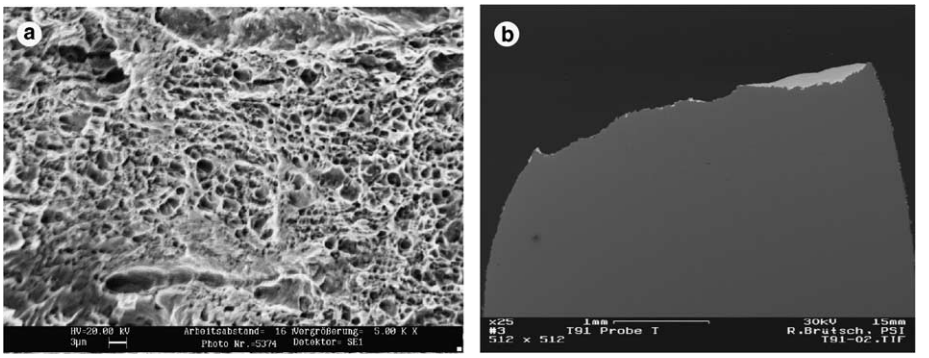

Fig. 4. SEM images of (a) fracture surface and (b) cross-section of T91 ruptured in LBE.

(ruptured with and without irradiation) shows a ductile fracture face without any brittle areas (compare Fig. 4(a)) and the typical necking for ductile materials has occurred (Fig. 4(b)).

4. Results obtained for test section no. 2 and discussion

Dissembling of the test section was performed in a hot cell. Visual inspection showed clearly that a leakage in the test section tube exists. Calculations performed with the ANSYS code give a clear explanation to the failure of the tube [15]. The maximum temperature of the outer surface of the tube was found to be about 780 °C, of the inner surface of about 67 °C. The temperature difference was estimated to be around 110 °C, which means that the thermal stress alone due to this temperature difference may reach about 170 MPa. The ultimate tensile strength for T91 is 101 MPa at 700 °C, and 41 MPa at 800 °C [20]. After about 140,000 cycles hence followed by the wobbling frequency of the beam (the leakage started at around 32 h), the crack propagated through the wall and resulted in a leakage. A quite huge amount of LBE was dropped out during operation before stopping the experiment and parts of it was used for analytical examination. Dissembling of the test section no. 2 in the hot cell is given in Fig. 5. The irradiated area in the test section tube is pointed out with an arrow. In Fig. 6 the irradiated part of the window with the crack in the footprint of the beam can be seen: Fig. 6(a) shows the outer surface and Fig. 6(b) the inner surface. The coloured pattern of the footprint (Fig. 6(a))

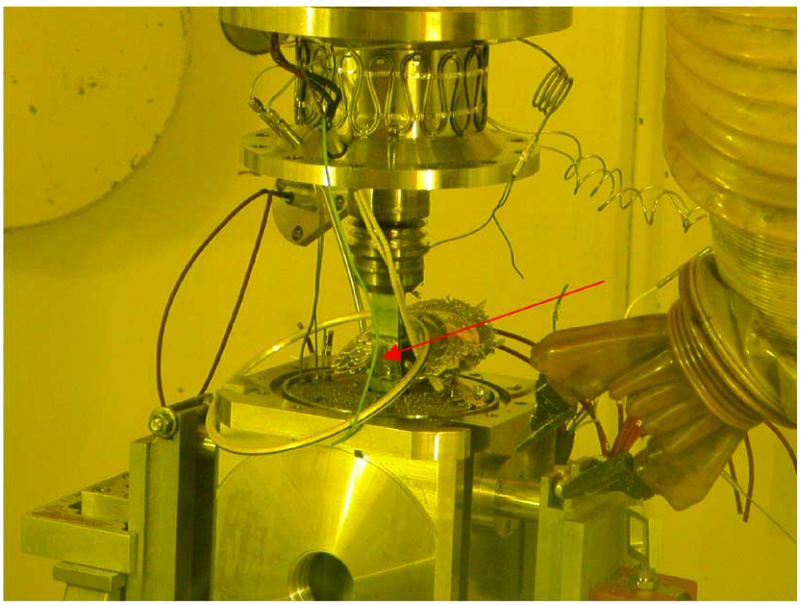

Fig. 5. Dissembling of the test section no. 2 in the hot cell. The arrow marks the irradiated area of the tube.

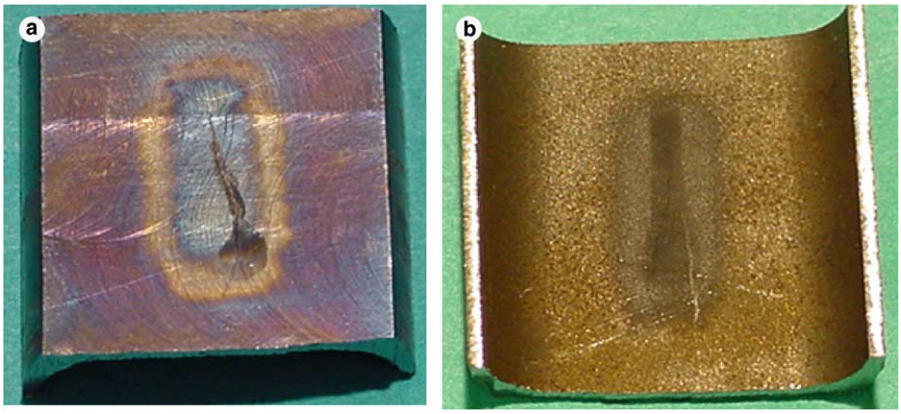

Fig. 6. Detailed examination along the crack was performed.

reflects nicely the temperature distribution achieved during irradiation.

4.1. Irradiated LBE

High-resolution α-spectroscopy was performed on the chemically separated solutions of irradiated LBE. Additionally calculations were made in order to compare them with the experimental results. In Table 2 the calculated values are opposed to the experimental ones. The analysis was carried out about half a year after the irradiations was stopped, thus only Po-isotopes could be analysed having a relatively long half-life time. Calculations taken the correct beam parameters into account revealed the generation of the Po-isotopes 202, 203, 204, 205 and 207. We believe that theses isotopes were present during and directly after irradiation but due to their short half-life times they were already decayed when the analysis was started. A comparison of the calculated and the experimental activities achieved for the Po isotopes 206 and 208 shows a good consistence of the values, whereas the estimation of the Po 210 activity is too low. The generation of the Po 210 isotope requires thermal neutrons and the FLUKA code has only included reactions with fast neutrons. It is definitely thinkable that during the irradiation a small amount of thermal neutrons is generated which are responsible for the formation of Po 210. For future calculations may be the FLUKA code has to be modified or another tool has to be used for performing these calculations.

Table 2
Values of Po isotopes revealed by neutronic calculation in comparison with the and experimental data

Isotope	Bq/calc.	Bq/g calc.	Bq/g exp.
^{202}Po	3.1×10^{9}	1.6×10^{4}	
^{203}Po	2.3×10^{11}	1.2×10^{6}	
^{204}Po	9.9×10^{11}	5.3×10^{6}	
^{205}Po	1.1×10^{12}	5.9×10^{6}	
^{206}Po	9.1×10^{10}	4.8×10^{5}	9.95×10^{5}
^{207}Po	7.9×10^{11}	4.2×10^{6}	
^{208}Po	5.9×10^{8}	3.1×10^{3}	4.8×10^{3}
^{210}Po	2.0×10^{6}	11	150

4.2. Inspection of the tube

The general feature of the crack can be characterized as brittle and ductile mixed fracture. Most of areas, particularly the central part, show brittle fracture (Fig. 7(a)). Only a small part near the outer surface and close to the upper end of the crack tip presents a typical ductile fracture mode (Fig. 7(b) lower part). This may indicate that the crack started at the inner surface and propagated to the outer surface. In the central part the crack could be promoted by irradiation and LBE embrittlement effects, which resulted in a brittle fracture. The ductile fracture part at the upper end of the crack is less than 200 μm thick and could be broken at a relative high speed like tearing. The crack starting at the inner surface of the tube is understandable because microcracks in the surface layer were ready to propagate under high tension stress induced by the temperature gradient. More details are given in [21].

4.3. Inspection of the specimen

The specimen was applied to 200 MPa tensile stress and, meanwhile, in the irradiation area a thermal stress of about 120 MPa was induced by the temperature gradient during irradiation. Under such a severe condition of high temperature, high stress and intensive irradiation, irradiation-assisted-stress-corrosion-cracking (IASCC) is very likely to occur. However, on the cross-sections in both directions perpendicular and parallel to the tensile axis there was not observed any

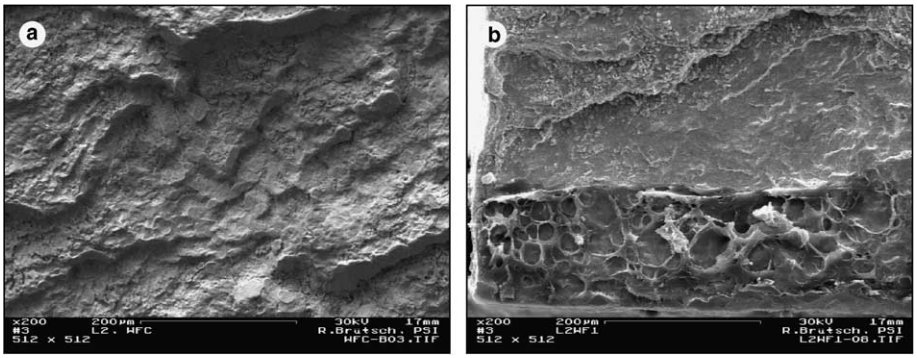

Fig. 7. Micrographs showing (a) brittle fracture in the central part and (b) ductile fracture in an area near the outer surface and close to the upper end of the crack.

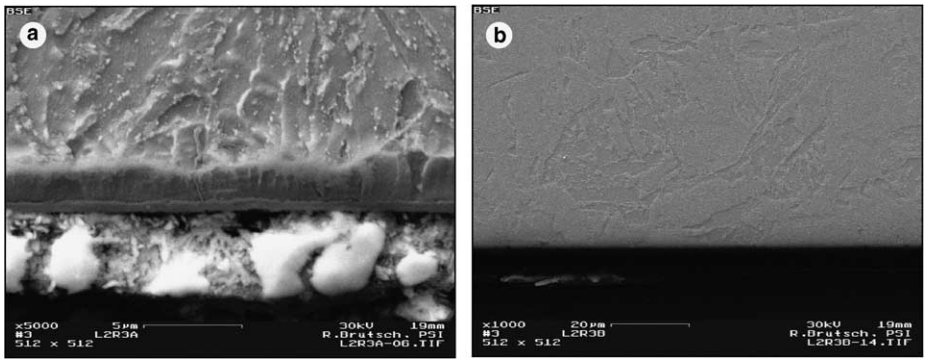

Fig. 8. Cross-section of the specimen (a) in the irradiated area and (b) in the non-irradiated area.

microcrack. Instead of microcracks, a thin oxide layer formed on the surface. The oxide layer up to a thickness of 3 μm thick was only revealed in the irradiated area (see Fig. 8(a)). Outside the irradiated area no oxide layer was observed (Fig. 8(b)). The formation of the oxide layer is believed due to the high temperature during irradiation. Further results obtained on the specimens were presented in [21].

5. Conclusions and outlook

Up to now four irradiation experiments have been performed in the LiSoR facility. Post-irradiation examinations have been done on the specimens and on the tubes of test section nos. 1 and 2. The irradiation of test section no. 1 was only 1 h. The inspection of two T91 tensile specimens ruptured with and without irradiation showed a ductile fracture face and no differences between both are observable due to the short irradiation period. Tensile tests will be performed on T91 material irradiated in LiSoR experiments nos. 2, 3 and 4 in the near future. The results obtained on test tube and specimen after irradiation in LiSoR no. 2 are the following:

(1) The LBE leakage was due to a crack formed in the irradiation zone of the tube. The crack should be mainly attributed to thermal fatigue induced by high thermal stress and partially due to surface microcracks.
(2) The fracture surfaces of the crack are dominated with brittle fracture features, which may assisted by LBE embrittlement effects.
(3) An oxide layer was formed at the irradiated area of the specimen whereas no oxidation has occurred beside the footprint of the beam. The high temperatures induced by the beam are responsible for the formation of the protecting oxide layer.

PIE on specimens and tubes irradiated in LiSoR experiments nos. 3 and 4 are planned to be performed soon. Additionally tensile tests will be done on irradiated material (tube and specimen) of the experiments nos. 2, 3 and 4.

Acknowledgement

The assistance of Mr T. Rebac for metallurgical examination and Dr D. Gavillet for micro hardness measurements is gratefully acknowledged. The authors especially wish to express their thanks to Mr V. Boutellier for his support by cutting out and preparing the specimens, Dr L. Zanini for performing the neutronic calculations and Dr J. Eikenberg for the analysis on irradiated LBE. The work has been performed in the framework of the MEGAPIE project and is partly supported by the BBW within the 5th EU frame work program.

References

[1] F. Barbier, A. Rusanov, J. Nucl. Mater. 296 (2001) 231.
[2] H. Glasbrenner, J. Konys, G. Müller, A. Rusanov, J. Nucl. Mater. 296 (2001) 237.
[3] C. Fazio, G. Benamati, C. Martini, G. Palombarini, J. Nucl. Mater. 296 (2001) 243.
[4] Several presentations presented during the III International Workshop on Material for Hybrid Reactors and related Technologies, Rome, 13–15 October 2003.
[5] M.H. Kamdar, Treatise Mater. Sci. Technol. 25 (1983) 361.
[6] M.G. Nicholas, C.F. Old, J. Mater. Sci. 14 (1979) 1.
[7] Y. Dai, in: Proceedings of ICANS-XIII and ESS-PM4, October 11–19, 1995, PSI, p. 604.
[8] R.L. Klueh, in: Proceedings of I International Workshop on Spallation Materials Technology, 23–25 April 1996, Oak Ridge, p. 3.
[9] G. Nicaise, A. Legris, J.B. Vogt, J. Foct, J. Nucl. Mater. 296 (2001) 256.
[10] T. Auger, G. Lorang, S. Guerin, J.L. Pastol, D. Gorse, in: Presented during the III International Workshop on Material for Hybrid Reactors and related Technologies, Rome, October 13–15, 2003.
[11] C. Fazio, I. Ricapito, G. Scaddozzo, G. Benamati, J. Nucl. Mater. 318 (2003) 325.
[12] H. Glasbrenner, F. Gröschel, T. Kirchner, J. Nucl. Mater. 318 (2003) 333.
[13] T. Kirchner et al., J. Nucl. Mater. 318 (2003) 70.
[14] S. Dementjev, H. Glasbrenner, T. Kirchner, F. Heinrich, I. Bucenieks, E. Platacis, A. Pozdnjaks, G. Kirshtein, Magnetohydrodynamics 37 (2001) 386.
[15] H. Glasbrenner, V. Boutellier, Y. Dai, S. Dementjev, F. Gröschel, L. Ni, D. Viol, Th. Kichner, PSI-Report TM 34-02-04, 2002.
[16] H. Glasbrenner, V. Boutellier, Y. Dai, S. Dementjev, F. Gröschel, D. Viol, PSI-Report TM 34-02-09, 2003.
[17] H. Glasbrenner, J. Eikenberg, F. Gröschel, L. Zanini, in: Presented during the III International Workshop on Material for Hybrid Reactors and related Technologies, Rome, 13–15 October 2003.
[18] A. Fasso, A. Ferrari, P.R. Sala, in: A. King, F. Barao, M. Nakagawa, L. Tavora, P. Vaz (Eds.), Proceedings of the MonteCarlo 2000 Conference, Lisbon, 23–26 October 2000, Springer-Verlag, Berlin, 2001, p. 159.
[19] F. Atchison, H. Schaal, ORIHET3-Version 1.12; A guide for users, Paul Scherrer Institut (2000).
[20] X. Jia, N. Baluc, PSI report AN-34-02-03, 2002.
[21] Y. Dai, H. Glasbrenner, V. Boutellier, R. Bruetsch, X. Jia, F. Groeschel, III International Workshop on Material for Hybrid Reactors and related Technologies, Rome, 13–15 October 2003.